Gravitational wave memory of gamma-ray burst jets

Norichika Sago,[1] Kunihito Ioka,[2] Takashi Nakamura,[3] and Ryo Yamazaki[1]

[1]*Department of Earth and Space Science, Graduate School of Science, Osaka University, Toyonaka 560-0043, Japan*
[2]*Physics Department, Pennsylvania State University, University Park, Pennsylvania 16802, USA*
[3]*Department of Physics, Kyoto University, Kyoto 606-8502, Japan*

Gamma-ray bursts (GRBs) are now considered as relativistic jets. We analyze the gravitational waves from the acceleration stage of the GRB jets. We show that (i) the point mass approximation is not appropriate if the opening half-angle of the jet is larger than the inverse of the Lorentz factor of the jet; (ii) the gravitational waveform has many step function like jumps, and (iii) the practical DECIGO and BBO may detect such an event if the GRBs occur in the Local Group. We found that the light curve of GRBs and the gravitational waveform are anticorrelated so that the detection of the gravitational wave is indispensable to determine the structure of GRB jets.

I. INTRODUCTION

The gravitational wave astronomy enters its first step. The ground-based laser interferometers such as TAMA300, LIGO and GEO600 have already begun operations covering 10 Hz–kHz band, and VIRGO will be also in operation soon. The Laser Interferometer Space Antenna (LISA) [1] covering $10^{-4} - 10^{-2}$ Hz is expected to be launched in 2011. Recently, in addition, the Decihertz Interferometer Gravitational wave Observatory (DECIGO), which aims the frequency band around decihertz ($10^{-2} - 10$ Hz), has been proposed [2]. The decihertz antenna is also considered in the NASA Roadmap Beyond Einstein and is called the Big Bang Observer (BBO) [3].

It might be possible to construct a practical DECIGO and BBO with $h_{\rm rms} \sim 3 \times 10^{-24}$ at ~ 0.1 Hz. Although this limiting sensitivity is $\sim 10^3$ times less than the ultimate quantum limit $h_{\rm rms} \sim 3 \times 10^{-27}$ at ~ 0.1 Hz for a 100 kg mirror mass, the practical DECIGO and BBO may achieve the following important results [2,4]: (1) The chirp signals of coalescing binary neutron stars at $z \sim 1$ may be detected with a signal-to-noise ratio (SNR) ~ 10 for 1 yr observation. (2) The time variation of the Hubble parameters of our universe may be determined by the chirp signals so that we can directly measure the acceleration of the expansion of the universe. (3) The stochastic gravitational waves from inflation may be detected if $\Omega_{\rm GW} \gtrsim 10^{-15}$, which is the upper limit from cosmic microwave background. (4) An arcminute position and an accurate (~ 0.1 s) coalescence time of the coalescing binary neutron stars at ~ 300 Mpc may be determined a week before the final merging, so that the all band electromagnetic detectors can perform the simultaneous follow-up observation. An accurate position may be also important for the reconstruction of the density distribution and the shape of the galactic dark halo [5–7].

In this paper, we consider gamma-ray bursts (GRBs) as possible sources of the gravitational waves for DECIGO and BBO. The GRBs are the most luminous objects in the universe. The recent discovery of the afterglow has revolutionized the understanding of the long duration GRBs (e.g. [8,9]). We are now confident that long GRBs with ~ 10 s duration eject relativistic flows with Lorentz factors $\gamma \gtrsim 100$ and the ejecta is collimated in a jet. This means that the nonspherical acceleration of a large mass is associated with GRBs. Therefore it is guaranteed that the GRB jet acceleration emits gravitational waves [10–12]. We will show that the typical frequency of the gravitational waves is about the inverse of the duration of GRBs ~ 0.1 Hz, so that the decihertz band of DECIGO and BBO best suits the detection of gravitational waves from the GRB jet (Sec. III).

Here we concentrate on the gravitational waves from the acceleration stage of GRB jets, while we also expect the gravitational waves from the formation of the central engine of GRBs [13–16] that could be detected by the ground-based laser interferometers. We know that the accelerated jet exists although we do not know how it is accelerated and what structure it has. Since the jet is accelerated near the central engine where the optical depth is quite large, the electromagnetic probe is useless. The high-energy neutrinos from GRBs ([17]) may provide a indirect probe of the central engine, while the gravitational waves may bring us the direct information of it. Thus the gravitational waves could be an ultimate way to see the acceleration regime.

The gravitational waves from the GRB jet have a "memory"; that is, the metric perturbation does not return to its original value at the end of the jet acceleration [18]. The gravitational wave memory is the change in the transverse-traceless (TT) part of the Coulomb-type ($\propto 1/r$) gravitational field generated by the masses of the system. These masses could be stars, neutrinos [19,20], gravitons [21–23], and in our case the GRB jets.

Segalis and Ori [10] analyzed the gravitational wave emitted when an ultrarelativistic blob is ejected from a massive object by using a point mass approximation. They

showed that the gravitational wave emission from such a source is antibeamed. This contrasts with the electromagnetic emission, which is beamed into the forward direction. They also obtained the detectable distance of about 15 Mpc and estimated the detection rate of about one per year by the advanced LIGO, assuming that the total energy of the GRBs is about $\sim 10^{52}$ erg and that GRBs follow supernovae.

On the other hand, recent studies suggest that the jet structure is essentially important for understanding the GRB phenomena [24–26]. Depending on the viewing angle, the structured jet model might be able to explain the diverse phenomena of GRBs, such as short GRBs, long GRBs, X-ray flashes (XRFs) and X-ray rich GRBs [27]. Here XRFs and X-ray rich GRBs are fast X-ray transients that are considered to be related to long GRBs [28]. Little is known about short GRBs since no afterglow was observed although many suggestions to show the similarity to long GRBs exist.

It is difficult to determine the jet structure only by the electromagnetic waves, since the photons are beamed into the forward direction and we can observe only a small angular portion $\sim \gamma^{-1} \sim 0.01$ rad of the whole jet. On the other hand, since the gravitational wave emission is antibeamed, it can be observed at larger viewing angles, so that we can see wider angular portion of the whole jet. Therefore the information carried by the gravitational waves is important to know the jet structure. In this paper we investigate the gravitational wave from an inhomogeneous jet. We model the inhomogeneous jet in which multiple subjets with a finite opening half-angle are ejected to various directions. The jet of GRBs should not be a single homogeneous one since a single explosion cannot produce a variable GRB. We discuss what kind of information is carried by the gravitational wave observed by DECIGO and BBO. We also discuss the detectability of such events.

This paper is organized as follows. In Sec. II, we consider the gravitational wave from a single jet acceleration. We investigate the angular dependence of the gravitational wave from a jet with a finite opening half-angle. In Sec. III, we discuss the gravitational waveform from the GRB jet adopting a unified model of the GRB proposed by some authors [27]. In Sec. IV, we calculate the strain amplitude detected by the gravitational wave detector. We also evaluate the maximum detectable distance to the GRBs for such events by using DECIGO and BBO. Finally, we summarize this paper and discuss our results in Sec. V. We use the geometric units $G = c = 1$ and the signature $(- + + +)$.

II. GRAVITATIONAL WAVE MEMORY OF A SINGLE JET

In this section we consider the gravitational waves from a single jet acceleration. Actually a single explosion

cannot produce a variable GRB. Many jets are to be ejected since the total duration of the burst is usually much longer than the variability timescale [29]. The many jets case will be discussed in the next section.

First let us remember the generic form of the gravitational wave memory [18,22]. We consider that the system consists of freely moving masses before and after the burst. Then the variation of the metric perturbation (which is the gravitational wave memory) is given by

$$\Delta h_{ij}^{\mathrm{TT}} = \Delta \sum_A \frac{4\gamma_A m_A}{r} \left(\frac{\beta_A^i \beta_A^k}{1 - \beta_A \cos\theta_A} \right)^{\mathrm{TT}}. \quad (1)$$

Here Δ means the difference between before and after the burst, m_A is the mass labeled by $A(= 1, 2, \cdots)$, r is the distance from the source to the observer, β_A^i is the velocity of mass A, $\gamma_A = (1 - \beta_A^2)^{-1/2}$ is the Lorentz factor of mass A, and θ_A is the angle between β_A^i and the direction from the source to the observer. Small Latin indices $(i, j, \cdots)$ run over spatial coordinates x, y, z, and the quantities r, β_A^i, θ_A are measured in the lab frame. The *TT* part of Δh_{ij} is obtained by $\Delta h_{ij}^{\mathrm{TT}} = P_{ik}P_{jl}\Delta h_{kl} - (1/2)P_{ij}(P_{kl}\Delta h_{kl})$ where $P_{ij} = \delta_{ij} - n_i n_j$ is the projection operator and n_i is the unit vector from the source to the observer [30]. The source quantities are to be evaluated at the retarded time.

The gravitational wave memory of a point mass acceleration is easily calculated from Eq. (1) [10–12]. Let us consider that a point mass M is accelerated to a Lorentz factor γ. Conservation of energy requires that the mass of the accelerated particle is $m = M/\gamma$. We take a coordinate such that the z axis is the direction from the source to the observer and $\beta^i \propto (\sin\theta \cos\phi, \sin\theta \sin\phi, \cos\theta)$. Then Eq. (1) gives the amplitude of the gravitational wave memory as

$$\Delta h \equiv \Delta h_+ + i\Delta h_\times = \frac{2\gamma m \beta^2}{r} \frac{\sin^2\theta}{1 - \beta\cos\theta} e^{2i\phi}, \quad (2)$$

where $\Delta h_+ \equiv \Delta h_{xx}^{\mathrm{TT}} = -\Delta h_{yy}^{\mathrm{TT}}$ and $\Delta h_\times \equiv \Delta h_{xy}^{\mathrm{TT}} = \Delta h_{yx}^{\mathrm{TT}}$ are two polarizations of the gravitational waves, plus and cross modes. For $\gamma \gg 1$ and $\theta \ll 1$, we have

$$|\Delta h| \simeq \frac{4\gamma m}{r} \frac{\theta^2}{\gamma^{-2} + \theta^2}, \quad (3)$$

while for $\gamma \gg 1$ and $\theta \gg \gamma^{-1}$

$$|\Delta h| \simeq \frac{2\gamma m}{r}(1 + \cos\theta). \quad (4)$$

Therefore the gravitational wave memory is antibeamed with a similar amplitude in almost all direction but little amplitude in the forward direction $\theta \lesssim \gamma^{-1}$. The waveform has a form like a step function. As we can see from Eq. (2), the rise time of the amplitude from its initial to final value is about the time to reach $\beta \sim 1$ if the energy γm is conserved. Thus the rise time is about $\delta t \sim 10^7$ cm/$c \sim 10^{-3}$ s in the fireball model of the GRBs

[31,32]. If a counter-jet exists [33], we sum both contributions to obtain

$$|\Delta h| = \frac{4\gamma m}{r} \sim 1.6 \times 10^{-22} \left(\frac{2\gamma m}{3 \times 10^{51} \text{ erg}} \right) \left(\frac{r}{1 \text{ Mpc}} \right)^{-1}, \tag{5}$$

for $\gamma \gg 1$ and $\theta \gg \gamma^{-1}$. (In this paper, however, we do not consider the counter-jet[1].)

In reality the opening half-angle of the GRB jet is larger than γ^{-1} [34,35]. Thus Eq. (2) is not appropriate for the GRB jet. To examine the effects of the finite opening half-angle let us first consider a simple model, that is, an uniform thin jet with an opening half-angle $\Delta\theta$ that is accelerated to a Lorentz factor γ. Since linear perturbation is additive, the gravitational wave memory of the GRB jet is given by

$$\Delta h = \int \frac{\sin\theta d\theta d\phi}{\Delta\Omega} H(\Delta\theta - |\theta - \theta_v|) H \left[\cos\phi \right.$$
$$\left. - \left(\frac{\cos\Delta\theta - \cos\theta_v \cos\theta}{\sin\theta_v \sin\theta} \right) \right] \Delta h_\bullet, \tag{6}$$

where $\Delta h_\bullet$ is the amplitude of a point mass in Eq. (2), $H(x)$ is the Heaviside step function describing that the jet is inside the cone, θ_v is the viewing angle that the jet axis (in the xz plane) makes with the z axis, and $\Delta\Omega = \int_0^{2\pi} \int_0^{\Delta\theta} \sin\theta d\theta d\phi = 2\pi(1 - \cos\Delta\theta) \simeq \pi(\Delta\theta)^2$ is the solid angle of the jet. Replacing ϕ with $-\phi$ in Eq. (6), we can show $\Delta h_- = 0$. For Δh_+ we can simplify Eq. (6) as

$$\Delta h_+ = \int_{\max[0,\theta_v - \Delta\theta]}^{\theta_v + \Delta\theta} d\theta \frac{2\gamma m \beta^2}{r\Delta\Omega} \frac{\sin^3\theta \sin 2\Delta\phi}{1 - \beta \cos\theta}, \tag{7}$$

where

$$\Delta\phi = \begin{cases} \pi: \Delta\theta > \theta_v \text{ and } 0 < \theta \le \Delta\theta - \theta_v, \\ \cos^{-1}\left[\frac{\cos\Delta\theta - \cos\theta_v \cos\theta}{\sin\theta_v \sin\theta} \right] \quad \text{:others.} \end{cases} \tag{8}$$

As in the point mass case, the gravitational waveform becomes like a step function, and the rise time of the amplitude is about the time to reach $\beta \sim 1$ if the energy γm is conserved.

In Fig. 1, the amplitude of the gravitational wave memory for the GRB jet in Eq. (7) is shown as a function of the viewing angle θ_v by solid lines. We adopt the Lorentz factor $\gamma = 100$. The opening half-angle of the jet is $\Delta\theta = 0.01, 0.1$ and 0.2 from top to bottom. We can see that, because of the antibeaming effect, the amplitude is suppressed in the forward direction, that is, when the
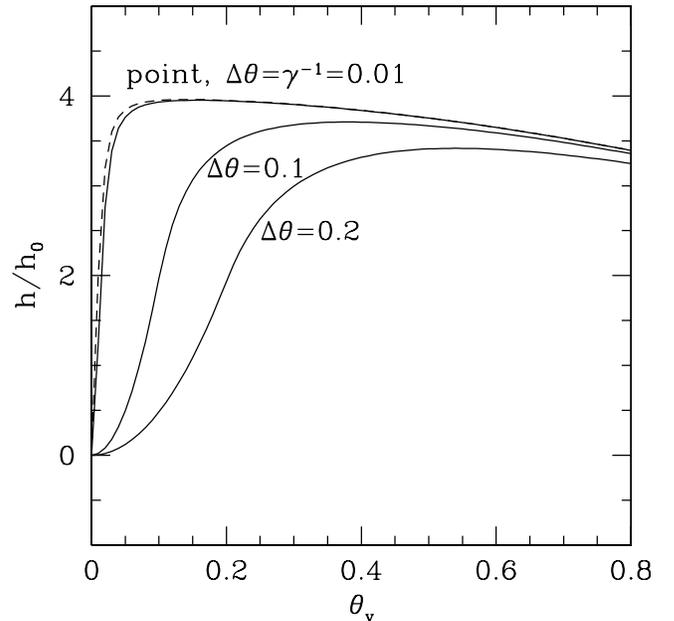
---

[1]From Eq. (2), we find that the ratio between the amplitude of the gravitational wave due to the forward jet and the one due to the counter-jet is $(1 + \beta \cos\theta_v)/(1 - \beta \cos\theta_v)$. Since we consider the case of $\theta_v \lesssim 0.25$ in this paper, this ratio is much larger than unity. Therefore we can neglect the effect of the counter-jet.

FIG. 1. The amplitude of the gravitational wave memory for the GRBs jet in Eq. (7) is shown as a function of the viewing angle θ_v by solid lines. We adopt the Lorentz factor $\gamma = 100$. The opening half-angle of the jet is $\Delta\theta = 0.01, 0.1$ and 0.2 from top to bottom. We can see that the amplitude is suppressed in the forward direction $\theta_v \lesssim \Delta\theta$. The amplitude for the point mass in Eq. (2) is also shown by the dashed line. Clearly the point mass approximation is good when the opening half-angle is smaller than the inverse of the Lorentz factor $\Delta\theta < \gamma^{-1}$ or the viewing angle is larger than the opening half-angle $\theta_v \gtrsim \Delta\theta$. The amplitude is normalized by $h_0 = \gamma m \beta^2/r \sim 2.7 \times 10^{-23}(\gamma m/10^{51} \text{ erg})(r/1 \text{ Mpc})^{-1}$.

viewing angle is smaller than the opening half-angle of the jet $\theta_v \lesssim \Delta\theta$. The amplitude of the memory for the point mass in Eq. (2) is also shown by the dashed line. We can find that the point mass is a reasonable approximation of the jet when the opening half-angle is smaller than the inverse of the Lorentz factor $\Delta\theta < \gamma^{-1}$ or the viewing angle is larger than the opening half-angle $\theta_v \gtrsim \Delta\theta$. The opening half-angle of the jet is usually small $\Delta\theta \sim 0.1$ [34,35] so that we observe the jet from off-axis direction usually. This means that the effects of the finite opening angle may not reduce the event rate of the gravitational waves from GRBs so much.

III. GRAVITATIONAL WAVEFORM FROM GAMMA-RAY BURST JETS

A. Typical frequency

The leading model of the GRB emission is the internal shock model [29]. The internal shock occurs in the relativistic wind when the fast moving flow catches up the slow one. The wind can be modeled by a succession of relativistic shells. A collision of two shells produces a

single pulse light curve, whose superposition makes a whole light curve.

When the GRB ejects many jets, the gravitational waveform from the GRB differs from a single step function, but has many steps since linear perturbation is additive. There are three timescales that determine the temporal structure of the gravitational wave memory of the GRB. The first is the rise time of the gravitational wave amplitude due to a single jet $\Delta T_{\rm rise}$. As argued in the previous section, $\Delta T_{\rm rise}$ is related to the acceleration time of the jet. The second is the separation between successive jets $\Delta T_{\rm sep} \sim 0.1$ s. The third is the total duration of the burst ΔT, which is about $\Delta T \sim 10$ s for long GRBs. Then the typical order between three timescales is

$$\Delta T_{\rm rise} \ll \Delta T_{\rm sep} \ll \Delta T. \tag{9}$$

Therefore the typical gravitational waveform should have many steps. Each step corresponds to the ejection of a jet, and the final amplitude of the gravitational wave memory is mainly determined by the total energy of the jets ejected from the GRB. The final amplitude is reached after the total duration ΔT. Thus the typical frequency in Fourier space of the gravitational waves is expected as

$$f_c \sim \frac{1}{\Delta T} \sim 0.1 \text{ Hz}. \tag{10}$$

This band is just the decihertz band of DECIGO and BBO.

B. A unified model of GRBs

Recently some of authors proposed a unified model of the GRBs [27]. In this model, the central engine of the long and short GRBs, XRFs and X-ray rich GRBs is the same, and the apparent differences come essentially from different viewing angles. We assume that the jet of the GRB consists of multiple subjets. These subjets have angular size of $\sim \gamma^{-1} \ll 0.1$ and are distributed within the whole GRB jet (~ 0.1). If many subjets point to our line of sight, the event looks like a long GRB, while if a single subjet points to us, it looks like a short GRB. If our line of sight is off-axis to any subjets, the event looks like an XRF or X-ray rich GRB.

An example of the subjet angular distribution is shown in Fig. 2, where $N_{\rm tot} = 350$ subjets are ejected for $\Delta T = 30$ sec and each subjet has $\gamma = 100$ and $\Delta \theta_{\rm sub} = 0.02$ rad. When we observe the source from the $\theta_\nu = 0$ axis (case "A"), we see spiky temporal structures [Fig. 3(a)] and may identify the case A as the long GRBs. When the line of sight is away from any subjets (cases "B.1" and "B.2"), soft and dim prompt emission, i.e., XRFs or X-ray rich GRBs are observed [Fig. 3(b)]. If the line of sight is inside an isolated subjet (case "C"), its observed pulse duration is much smaller than the case A [Fig. 3(c)], so that we may observe the short GRB. The
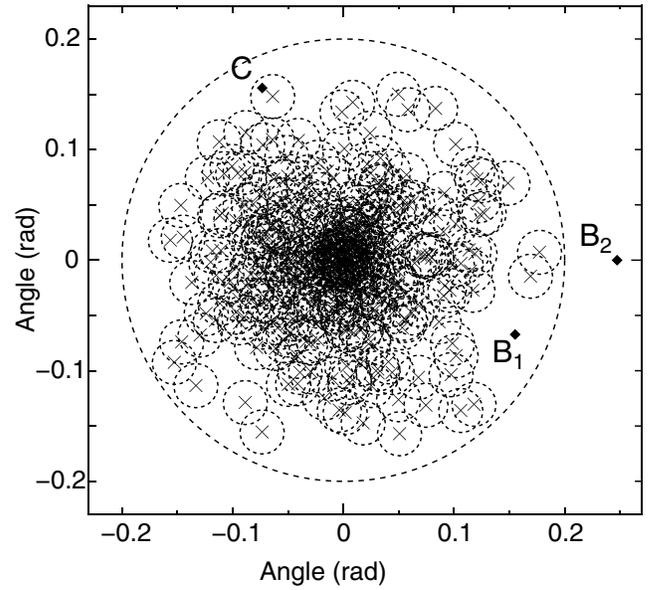

FIG. 2. The angular distribution of $N_{\rm tot} = 350$ subjets confined in the whole GRB jet in our simulation. The whole jet has the opening half-angle of $\Delta \theta_{\rm tot} = 0.2$ rad, while the subjets have $\Delta \theta_{\rm sub} = 0.02$ rad. The axes and the angular size of subjets are represented by crosses and the dotted circles, respectively. A represents the center of the whole jet and is hidden by the lines of subjets. (Also refer to Yamazaki, Ioka and Nakamura [27].)

details about the calculations of the X-ray and gamma-ray light curves in Fig. 3 are given in [27].

In Fig. 4, we show the plus mode of the gravitational wave as a function of time assuming the same model as above. Each panel (A, "B.1", "B.2" and C) corresponds to
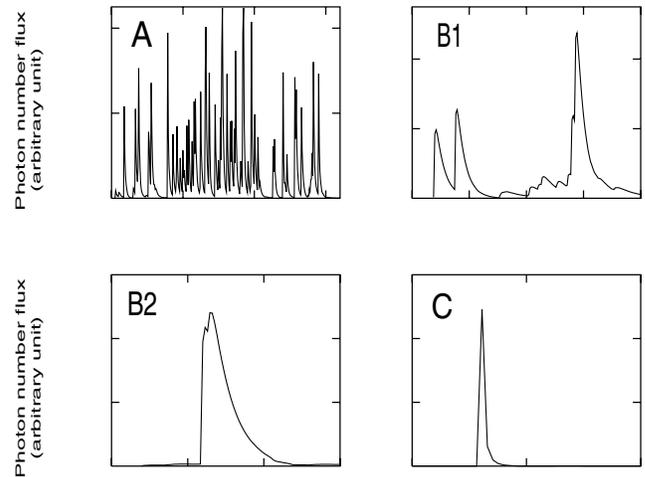

FIG. 3. The observed X-ray and gamma-ray photon number flux from the multiple subjets, corresponding the cases A (the upper left), "B.1" (the upper right), "B.2" (the lower left) and C (the lower right) in Fig. 2. Here the flux in $30 - 400$ keV band for each case is shown. (Also refer to Yamazaki, Ioka and Nakamura [27].)
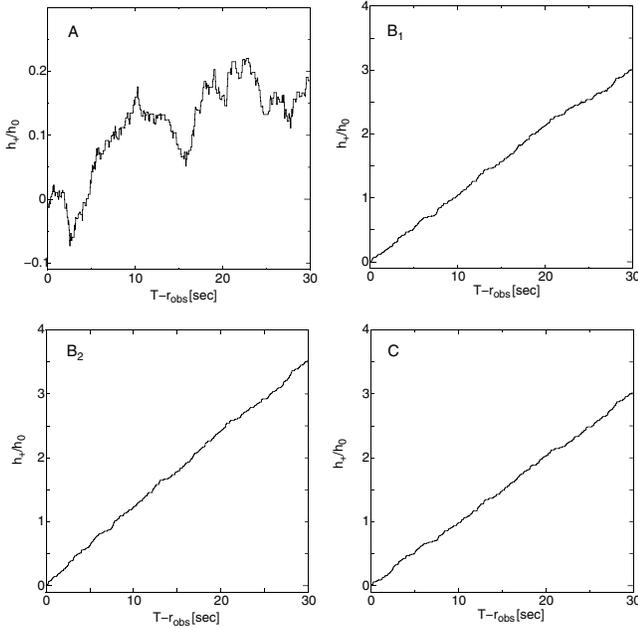
FIG. 4. The waveform of the gravitational wave memory from the GRB is shown. There are three timescales that determine the temporal structure of the waveform, the total duration $\Delta T \sim 30$ s, the separation between successive jets $\Delta T_{sep} \sim \Delta T/N_{tot} = 0.086$ s and the rise time of the amplitude due to a single jet $\Delta T_{acc} \sim 10^{-3}$ s (although we neglect the rise time here). The final amplitude is reached after the total duration ΔT. The normalization, h_0 is the same one in Fig. 1.

the viewing angle presented in Fig. 2 and the X-ray and gamma-ray light curves in Fig. 3. From Fig. 1 for $\Delta\theta \sim \gamma^{-1}$, the point mass approximation is good. Since $\Delta\theta_{sub} = 2\gamma^{-1}$ in our case we use the point mass approximation for each subjet and neglect the rise time of the amplitude, for simplicity. Each step corresponds to the ejection of a subjet, and the whole gravitational waveform has $N_{tot} = 350$ steps. Since the subjets are ejected for $\Delta T = 30$ sec, the final amplitude is reached after the duration ΔT.

We find that the final amplitude in case A is much smaller than the other cases and goes up and down more frequently than the others. This is because each memory of the subjet is proportional to $e^{2i\phi}$ from Eq. (2) and the distribution of ϕ is nearly isotropic for an on-axis observer like case A so that each memory tends to be canceled. On the other hand, if the viewing angle is large, the distribution of ϕ is not isotropic and either of two polarizations dominates the other one. Therefore, the amplitudes in cases "B.1";"B.2" and C increase monotonously. In addition, their waveforms resemble each other because the gravitational wave emitted by each subjet is nearly isotropic $\propto (1 + \cos\theta)$ for $\theta \lesssim 0.2$.

Comparing the gravitational waveform with the gamma-ray one in Fig. 3, we can see that the gravitational

wave amplitude is roughly anticorrelated with the photon flux. In case A, the gamma-ray is strong while the gravitational wave is weak. In cases "B.1" and "B.2", the gamma-ray is weak while the gravitational wave is strong so that we may confirm the existence of many off-axis subjets which are not identified by the gamma-ray. In case "'C", the gamma-ray is short and strong while the gravitational wave is long and strong. This means that the gravitational waves carry information on the off-axis jets. Thus, the gravitational waves are indispensable to explore the structure of the jet. For instance, in other models of the XRFs, emission comes from on-axis jets, so that the gravitational wave would have less amplitude. In other words, the gravitational wave can be used to verify or refute models of GRBs including our unified model of GRBs.

IV. DETECTABLE DISTANCE

For the detector with a peak sensitivity h_{peak} at frequency f_{peak}, the optimal sensitivity to the gravitational wave memory is $\sim h_{peak}$ as long as the rise time of the memory t_m is smaller than $\sim 1/f_{peak}$ [18,22]. For example, we consider a simple waveform as follows:

$$h(t) = \begin{cases} 0 & : t < 0, \\ \Delta h_m(t/t_m) & : 0 < t < t_m, \\ \Delta h_m & : t > t_m, \end{cases} \qquad (11)$$

which we call the slope waveform. We can calculate the Fourier component of this waveform, $\tilde{h} = \int_{-\infty}^{\infty} h(t)e^{i2\pi ft}dt$, which yields[2]

$$|\tilde{h}|^2 = \frac{(\Delta h_m)^2}{8\pi^4 f^4 t_m^2}(1 - \cos 2\pi f t_m). \qquad (12)$$

Note that $|\tilde{h}|^2 \simeq (\Delta h_m/2\pi f)^2$ for $f \ll 1/t_m$. In Fig. 5, we plot the characteristic amplitude of the gravitational wave memory, $h_c(f) = 2f|\tilde{h}|$ for $t_m = 30$ sec by the dashed line. We find that $h_c(f)$ is constant at $f \lesssim 1/t_m$, while it decreases for $f \gtrsim 1/t_m$. Therefore the detector has the maximal sensitivity h_{peak} for the gravitational wave memory as long as $1/t_m \lesssim f_{obs}$. We also plot $h_c(f)$ for the multiple step waveform (case "B.2") by the solid line. Here we fix the total energy and the distance of the source as $2m\gamma = 3 \times 10^{51}$ erg and 1 Mpc, respectively. For this case, the amplitude is larger than that for the slope waveform at $f \gtrsim 1/\Delta T$. This is because the waveform in the subjet model has the smaller timescale, ΔT_{sep}.

---

[2]Note that $\int_{-\infty}^{\infty} e^{i2\pi ft}H(t)dt = (1/2)[\delta(f) + Pv(i/\pi f)]$ where Pv denotes the principal value.
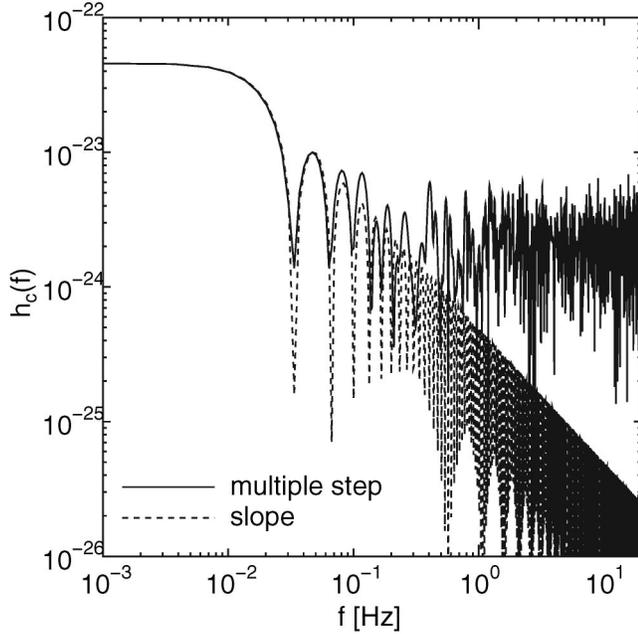
FIG. 5.   The characteristic amplitude h_c of the gravitational wave memory is plotted as a function of frequency for the whole GRB jets. The solid line represents h_c for the multiple step waveform (case "B.2") with the total energy $2\gamma m = 3 \times 10^{51}$ erg, the duration $\Delta T = 30$ sec and the distance to the source $r = 1$ Mpc. The dashed line represents h_c for the slope waveform with the duration $t_m = 30$ sec. Here the amplitude Δh_m in Eq. (11) is chosen so that both amplitudes coincide in the low-frequency limit.
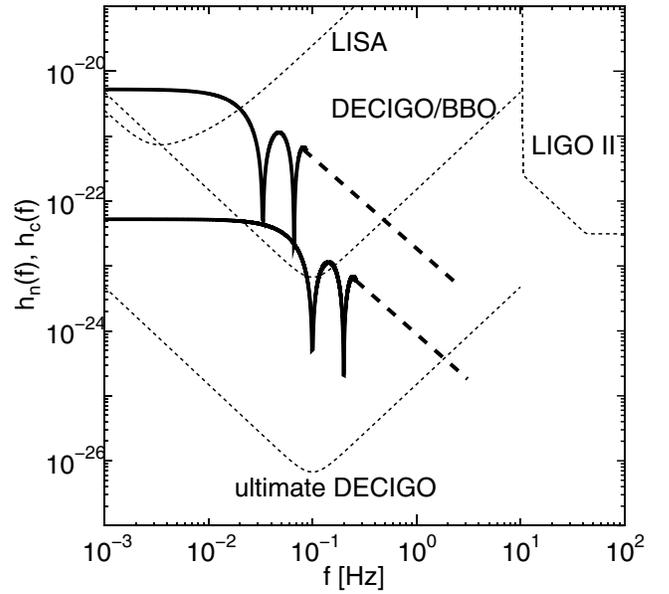

FIG. 6.   The noise amplitude h_n of LIGO II, LISA and DECIGO/BBO is also plotted by the dotted line. The characteristic amplitude for the gravitational wave memory of GRBs is also plotted by the bold solid line. The upper bold solid line corresponds to a GRB with the total energy $2\gamma m = 3 \times 10^{51}$ erg, the duration $\Delta T = 30$ sec at the 10 kpc, and the lower one to a GRB with $2\gamma m = 3 \times 10^{51}$ erg , $\Delta T = 10$ sec at the 1 Mpc. The characteristic amplitude for the slope waveform with $\Delta h_m = 4m\gamma\beta^2/r$ is used for the low-frequency region, $f \lesssim 1/\Delta T$. The amplitude at $f \gtrsim 1/\Delta T$ (plotted by the bold dashed line) depends on the structure of the GRB jet. The SNR can be obtained by Eq. (13).

In Fig. 6, we plot the noise amplitude $h_n(f) = [5fS_h(f)]^{1/2}$ for LIGO II, LISA and DECIGO/BBO[3], where $S_h(f)$ is the spectral density of the detector's strain noise at frequency f, and five comes from sky-averaging [38]. We also plot the characteristic amplitude of the gravitational wave memory by the bold line. For the low-frequency region, $f \lesssim 1/\Delta T$, we use the result for the slope waveform with $\Delta h_m = 4m\gamma\beta^2/r$, while we plot it by the bold dashed line in the high-frequency region, $f \gtrsim 1/\Delta T$, because it depends on the structure of the GRB jet. The upper bold line corresponds to a GRB with $(\Delta T, r, 2\gamma m) = (30 \text{ sec}, 10 \text{ kpc}, 3 \times 10^{51} \text{ erg})$, and the lower one to a GRB with $(\Delta T, r, 2\gamma m) = (10 \text{ sec}, 1 \text{ Mpc}, 3 \times 10^{51} \text{ erg})$. The signal-to-noise ratio (SNR) is given by

$$\text{SNR}^2 = \int_0^\infty d(\ln f) \frac{h_c(f)^2}{h_n(f)^2}; \qquad (13)$$

thereby one can roughly read off the SNR from Fig. 6. When the duration of GRBs is shorter than 10 sec, the detectable distance reaches the Local Group (~ 1 Mpc) by using the practical DECIGO and BBO. On the other hand, the detectable distance is reduced when the duration is longer than 10 sec. If a GRB happens in our galaxy, we can get the information on the high-frequency region $f \gtrsim 1/\Delta T$. This may make it possible for us not only to detect the gravitational wave memory, but also to extract important information about the structure of the GRB jet from the observed gravitational wave.

V. SUMMARY AND DISCUSSION

In this paper, we have investigated the gravitational wave emitted in the acceleration phase of the GRB jet. At first, we have considered the angular distribution of a GRB jet with a finite opening half-angle $\Delta\theta$. As a result, we have shown that we can deal with the jet as a point mass if the opening half-angle is smaller than the inverse of the Lorentz factor, γ^{-1}, or the viewing angle θ_v is larger than the opening half-angle. We have also shown that the gravitational radiation is weak in the angular size $\sim \gamma^{-1}$. Next, we have considered the waveform of the

---

[3]The LIGO II noise curve is taken from [36]. We adopt $S_h(f) = 1.22 \times 10^{-51}f^{-4} + 2.11 \times 10^{-41} + 1.22 \times 10^{-37}f^2$ Hz^{-1} for LISA [37], and $S_h(f) = 4.5 \times 10^{-51}f^{-4} + 4.5 \times 10^{-45}f^2$ Hz^{-1} for DECIGO/BBO [2], where f is in unit of Hz.

gravitational wave from the GRBs. We have found that many steps usually appear in the waveform. This has been explicitly shown for the multiple subjet model of GRBs. If we observe the GRBs from the front, the observed amplitude of the gravitational wave is suppressed because the wave from each subjet tends to cancel one another. On the other hand, the amplitude increases monotonously for the off-axis observer. In addition, we have considered the detectability of GRBs by using the practical DECIGO and BBO. We have found that we may detect the gravitational wave emitted from the GRB jet if it locates within 1 Mpc.

Since the gravitational wave memory is antibeamed, almost all GRBs detected by the gravitational waves will be observed with off-axis viewing angle. The photon emission from such off-axis GRBs is softer and dimmer than the on-axis ones due to the relativistic beaming [39,40]. Therefore the GRBs detected by the gravitational wave memory may be observed as XRFs [41,42] or rather softer events in the UV/optical bands [33]. The prompt electromagnetic emission is too dim to be observed in the case of large viewing angle. Even then, bright radio afterglows can be seen several months after the GRB explosion since the relativistic beaming effect becomes weak [43,44]. The association with a bright radio source might help us to identify the signal of the gravitational wave memory. In addition, the association with supernovae observed in the optical band may be also helpful. XRFs may be GRBs with large viewing angles [27,40]. The gravitational waves will be observed prior to the XRFs with the time delay being longer for softer and dimmer XRFs [39]. Thus the gravitational waves allow one to test the off-axis GRB model for the XRFs.

Unfortunately the event rate of the gravitational waves associated with the detectable GRBs may be small. Since the true GRB rate is estimated as ~ 250 Gpc^{-1}yr^{-1} [34], the event rate within the detectable distance ~ 1 Mpc (see Sec. IV) is only 3×10^{-7} yr^{-1}; that is very small compared with the detection rate of the gravitational wave by the central engine [45]. However the gravitational wave event rate without detectable GRBs could be much higher. Recently, many observations support a massive stellar origin for the long GRB [8,9] and it is widely assumed that a massive collapsing star ("collapsar") is the progenitor [46,47]. Suppose the GRB jets have the same total

energy. Although the GRB jet cannot break through the star because of weak collimation or it is baryon-loaded, so that $2 \lesssim \gamma \lesssim 30$, the resultant gravitational wave may have same amplitude as usual succeeded GRBs. Hence the detection rate of such events may be improved. Furthermore we calculate the detection rate for mean events. However the total energy is distributed around these mean values. Then the detections will be dominated by rare, energetic events. For instance, even if only $\sim 2\%$ events are 10 times more energetic, the detection rate will be increased by $\sim 2\% \times 10^3 \sim 20$, since we can observe 10 times farther events. Even if we take account of the above, the detection rate is 6×10^{-3} yr^{-1} optimistically. We need ~ 10 times better sensitivity than that of practical DECIGO/BBO for the detection rate ~ 1 yr^{-1}.

The gravitational wave memory does not depend on the form of energy. For example, even if the jet starts out as a pure Poynting flux jet [17,48], the memory is observed in the similar way. One may also think that the memory is lost if the jet is decelerated, for example, at the internal shock, the external shock and the termination shock inside the massive star. However at the internal and external shock almost all kinetic energy of the jet goes into the photon emission whose memory also remains. (In Eq. (1), γm should be interpreted as the photon energy, and the photon speed β must be set to 1.) Thus the amplitude of the gravitational wave memory does not change so much. At the termination shock between the jet and the massive stellar envelope, the kinetic energy may be converted to the neutrino emission [49,50]. Since the neutrino also leave the memory, the gravitational wave memory may not be reduced so much as long as the cooling is not severe in the jet head [50]

[1] http://lisa.jpl.nasa.gov/index.html.
[2] N. Seto, S. Kawamura, and T. Nakamura, Phys. Rev. Lett. **87**, 221103 (2001).
[3] http://universe.gsfc.nasa.gov/.
[4] R. Takahashi and T. Nakamura, Astrophys. J. **596**, L231 (2003).
[5] K. Ioka, T. Tanaka, and T. Nakamura, Astrophys. J. **528**, 51 (2000).
[6] K. Ioka, T. Tanaka, and T. Nakamura, Phys. Rev. D **60**, 083512 (1999).
[7] K. Ioka, T. Chiba, T. Tanaka, and T. Nakamura, Phys. Rev. D **58**, 063003 (1998).

[8] P. Meszaros, Annu. Rev. Astron. Astrophys. **40**, 137 (2002).

[9] B. Zhang and P. Meszaros, Int. J. Mod. Phys. A **19**, 2385 (2004).

[10] E. B. Segalis and A. Ori, Phys. Rev. D **64**, 064018 (2001).

[11] T. Piran, astro-ph/0102315.

[12] T. Piran, gr-qc/0205045.

[13] S. Kobayashi and P. Meszaros, Astrophys. J. **585**, L89 (2003).

[14] S. Kobayashi and P. Meszaros, Astrophys. J. **589**, 861 (2003).

[15] M. H. P. van Putten, A. Levinson, H. K. Lee, T. Regimbau, M. Punturo, and G. M. Harry, Phys. Rev. D **69**, 044007 (2004).

[16] C. L. Fryer, S. E. Woosley, and A. Heger, Astrophys. J. **550**, 372 (2001).

[17] A. Levinson and D. Eichler, Astrophys. J. **594**, L19 (2003).

[18] V. B. Braginsky and K. S. Thorne, Nature **327**, 123 (1987).

[19] R. Epstein, Astrophys. J. **223**, 1037 (1978).

[20] M. S. Turner, Nature **274**, 565 (1978).

[21] D. Christodoulou, Phys. Rev. Lett. **67**, 1486 (1991).

[22] K. S. Thorne, Phys. Rev. D **45**, 520 (1992).

[23] A. G. Wiseman and C. M. Will, Phys. Rev. D **44**, 2945 (1991).

[24] E. Rossi, D. Lazzati, and M. J. Rees, Mon. Not. R. Astron. Soc. **332**, 945 (2002).

[25] B. Zhang and P. Meszaros, Astrophys. J. **571**, 876 (2002).

[26] B. Zhang, X. Y. Dai, N. M. Lloyd-Ronning, and P. Meszaros, Astrophys. J. **601**, L119 (2004).

[27] R. Yamazaki, K. Ioka, and T. Nakamura, Astrophys. J. **607**, L103 (2004).

[28] J. Heise et al., in *Proc. in Gamma-Ray Bursts in the Afterglow Era*, edited by E. Costa, F. Frontera, and J. Hjorth (Spuringer, Berlin, 2001); T. Sakamoto *et al.*, Astrophys. J. **602**, 875 (2004).

[29] S. Kobayashi, T. Piran, and R. Sari, Astrophys. J. **490**, 92 (1997).

[30] C. W. Misner, K. S. Thorne, and J. A. Wheeler, *Gravitation* (Freeman, San Francisco, 1973).

[31] B. Paczynski, Astrophys. J. **308**, L43 (1986).

[32] J. Goodman, Astrophys. J. **308**, L47 (1986).

[33] R. Yamazaki, K. Ioka, and T. Nakamura, Astrophys. J. **591**, 283 (2003).

[34] D. A. Frail *et al.*, Astrophys. J. **562**, L55 (2001).

[35] J. S. Bloom, D. A. Frail, and S. R. Kulkarni, Astrophys. J. **594**, 674 (2003).

[36] E. E. Flanagan and S. A. Hughes, Phys. Rev. D **57**, 4535 (1998).

[37] L. S. Finn and K. S. Thorne, Phys. Rev. D **62**, 124021 (2000).

[38] K. S. Thorne, in *300 Years of Gravitation*, edited by S. W. Hawking and W. Israel (Cambridge University Press, Cambridge, England, 1987).

[39] K. Ioka and T. Nakamura, Astrophys. J. **554**, L163 (2001).

[40] R. Yamazaki, K. Ioka, and T. Nakamura, Astrophys. J. **606**, L33 (2004).

[41] R. Yamazaki, K. Ioka, and T. Nakamura, Astrophys. J. **571**, L31 (2002).

[42] R. Yamazaki, K. Ioka, and T. Nakamura, Astrophys. J. **593**, 941 (2003).

[43] A. Levinson, E. Ofek, E. Waxman, and A. Gal-Yam, Astrophys. J. **576**, 923 (2002).

[44] T. Totani and A. Panaitescu, Astrophys. J. **576**, 120 (2002).

[45] M. H. P. van Putten and A. Levinson, Astrophys. J. **584**, 937 (2003).

[46] S. E. Woosley, Astrophys. J. **405**, 273 (1993).

[47] B. Paczynski, Astrophys. J. **494**, L45 (1998).

[48] M. Lyutikov and R. D. Blandford, astro-ph/0312347.

[49] P. Meszaros and E. Waxman, Phys. Rev. Lett. **87**, 171102 (2001).

[50] S. Razzaque, P. Meszaros, and E. Waxman, Phys. Rev. D **69**, 023001 (2004).